T.R.
BOLU ABANT İZZET BAYSAL UNIVERSITY
INSTITUTE OF GRADUATE STUDIES
Department of Physics

EFFECT OF FABRICATION PARAMETERS ON STRUCTURAL AND ELECTRICAL PROPERTIES OF MgB_2 SAMPLE

DOCTOR OF PHİLOSOPHY

DİNÇER YEĞEN

ACADEMIC SUPERVISOR
Prof. Dr. Cabir TERZİOĞLU

BOLU, AĞUSTOS - 2022

APPROVAL OF THE THESIS

Effect Of Fabrication Parameters On Structural And Electrical Properties of MgB_2 Sample submitted by **Dinçer YEĞEN** and defended before the Examining Committe Members listed below in partial fulfillment of the requirements for the degree of **Doctor of Philosophy** in **Department of Physics, Institute of Graduate Studies of Bolu Abant Izzet Baysal University in 22.08.2022** by

Examining Committee Members	**Signature**
Supervisor Prof. Dr. Cabir TERZİOĞLU Bolu Abant İzzet Baysal University	....
Member Prof. Dr. Osman GÖRÜR Bolu Abant İzzet Baysal University	....
Member Doç. Dr. Sedat ÇETİN Bolu Abant İzzet Baysal University	....
Member Prof. Dr. Muharrem GÖKÇEN Düzce University	....
Member Prof. Dr. Özgür ÖZTÜRK Kastamonu University	....

Prof. Dr. İbrahim KÜRTÜL

Director of Instıtute of Graduate Studies

ETHICAL DECLARATION

In this thesis dissertation that was properly prepared according to the Thesis Writing Rules of Bolu Abant İzzet Baysal University of the Institute of Graduates Studies, I hereby declare that;

- All data, information, and documents presented in the thesis were obtained in accordance with the academic and ethical rules,
- All data, documents, assessments, and results were presented in accordance with the scientific ethical and moral rules,
- All works that were benefitted in the thesis were appropriately cited,
- No alteration was made in the data used,
- Study presented in this thesis is original,

Otherwise, I declare that I accept the loss of all my rights in case any contradiction that may arise against me.

Based on the plagiarism report that was generated on the date of 25/08/2022 by using predetermined filtrations set by Directorate of Institute of Graduate Studies of the Turnitin programme, a plagiarism detection sofware, the similarity index detected was 28%.

____

Dinçer YEĞEN

ABSTRACT

EFFECT OF FABRICATION PARAMETERS ON STRUCTURAL AND ELECTRICAL PROPERTIES OF MgB_2 SAMPLE
PHD THESIS
DİNÇER YEĞEN
BOLU ABANT IZZET BAYSAL UNIVERSITY
INSTITUTE OF GRADUATE STUDIES
DEPARTMENT OF PHYSICS
(SUPERVISOR: PROF. DR. CABİR TERZİOĞLU)

BOLU, AUGUST 2022
LIV + 54 PAGES

In this thesis, the effects of annealing temperature on the microstructure, electrical and magnetic properties of MgB_2 samples during the annealing process were investigated. For this purpose, 4 different samples (S650, S750, S850 and S950) were produced by pressing MgB_2 in powder form into bulk and annealing at 650°C, 750°C, 850°C and 950°C for 1 hour. In order to compare the produced samples, XRD, SEM, R-T, R-H and AC susceptibility measurements were taken. When XRD measurements were examined, in addition to obtaining information about their purity, crystal structure parameters *a* and *c* (crystal structure size) were calculated. By examining the surface structures from SEM measurements, particle sizes and material densities were calculated. The temperatures at which MgB_2 samples, a typical Type-II superconductor, started to become superconducting (T_{onset}) and completely superconducting (T_{offset}) under different external magnetic fields were determined from the measurements of the change in resistance with respect to temperature. In these measurements, the H_{c1} magnetic fields, at which temperatures the external magnetic fields we determined, began to deteriorate the superconductivity, and the H_{C2} magnetic fields, which completely deteriorated, were determined. In the R-H measurements, the curves of the variation of the resistance with externally applied DC magnetic field at constant temperature were obtained. From these curves, the H_{C2} magnetic fields, which are completely disrupted by superconductivity at constant temperature, were found. T_{onset} and T_{offset} temperatures were determined from the curves obtained from AC-Susceptibility measurements, and J_c intergranular critical current densities were calculated.
As a result of all measurements and calculations; The increase in annealing temperature up to 850°C improves the microstructure properties such as grain size, surface density, intergranular bonding, and worsens after this temperature, the critical temperature, critical current density and critical magnetic fields are better in the S850 sample, all measurements are compatible and consistent with each other, and showed that 850°C temperature in heat treatment of all measurements improved the microstructure, surface morphology, superconductivity and magnetic properties of the MgB_2 sample.

KEYWORDS: MgB_2, Microstructure, XRD, SEM, AC-Susceptibility

ÖZET

İMALAT PARAMETRELERİNİN MgB_2 NUMUNESİNİN YAPISAL VE ELEKTRİKSEL ÖZELLİKLERİNE ETKİSİ
DOKTORA TEZİ
DİNÇER YEĞEN
BOLU ABANT İZZET BAYSAL ÜNİVERSİTESİ
LİSANSÜSTÜ EĞİTİM ENSTİTÜSÜ
FİZİK ANABİLİM DALI
(TEZ DANIŞMANI: Prof. Dr. CABİR TERZİOĞLU)

BOLU, AĞUSTOS - 2022
LIV – 54 SAYFA

Bu tezde, MgB_2 numunelerinin süperiletken hale getirilirken yapılan tavlama işlemi sırasında tavlama sıcaklığının mikroyapı, elektrik ve manyetik özelliklerine etkileri incelenmiştir. Bu amaçla toz haldeki MgB_2 presslenerek bulk hale getirilip 650°C, 750°C, 850°C ve 950°C sıcaklıklarda 1 saat tavlanarak 4 ayrı numune (S650, S750, S850 ve S950) üretildi. Üretilen numunelerin karşılaştırılması amacıyla XRD, SEM, R-T, R-H ve AC alınganlık ölçümleri alındı. XRD ölçümleri incelendiğinde saflıkları hakkında bilgi edinilmesinin yanı sıra kristal yapı parametreleri *a* ve *c*'de (kristal yapı büyüklüğü) hesaplandı. SEM ölçümlerinden yüzey yapıları incelenerek tane büyüklükleri ve malzeme yoğunlukları hesaplandı. Direncin sıcaklığa göre değişim ölçümlerinden tipik bir Tip-II süperiletken olan MgB_2 numunelerinin farklı dış manyetik alanlar altında süperiletken olmaya başladığı (T_{onset}) ve tamamen süperiletken olduğu (T_{offset}) sıcaklıklar belirlendi. Bu ölçümlerde belirlediğimiz dış manyetik alanların hangi sıcaklıklarda süperiletkenliği bozmaya başladığı H_{C1} ve tamamen bozduğu H_{C2} manyetik alanları tespit edildi. R-H ölçümlerinde, sabit sıcaklıkta direncin dışardan uygulanan DC manyetik alanla değişim eğrileri elde edildi. Bu eğrilerden sabit sıcaklıkta süperiletkenliğin tamamen bozduğu H_{C2} manyetik alanları bulundu. AC-Alınganlık ölçümlerinden elde edilen eğrilerden T_{onset} ve T_{offset} sıcaklıklar belirlendi ve J_c taneler arası kritik akım yoğunlukları hesaplandı.

Tüm ölçümler ve hesaplamalar sonucunda; tavlama sıcaklığındaki 850°C kadar olan artışın tane boyutu, yüzey yoğunluğu, taneler arası bağlanma gibi mikroyapı özelliklerini iyileştirdiği bu sıcaklıktan sonra kötüleştiği, kritik sıcaklık, kritik akım yoğunluğu ve kritik manyetik alanların S850 numunede daha iyi olduğu, tüm ölçümlerin birbiriyle uyumlu ve tutarlı olduğu ve tüm ölçümlerin ısıl işlemde 850°C sıcaklığının MgB_2 numunesinin mikroyapısını, yüzey morfolojisini, süper iletkenliğini ve manyetik özelliklerini iyileştirdiğini gösterdi.

ANAHTAR KELİMELER: MgB_2, Mikroyapı, XRD, SEM, AC Alınganlık

TABLE OF CONTENTS

LIST OF FIGURES

Page

LIST OF TABLES

Page

LIST OF PICTURES

Page

LIST OF ABBREVIATIONS AND SYMBOLS

AC **:** Alternating current

C **:** Celcius

BCS Theory **:** Bardeen–Cooper–Schrieffer theory

DC **:** Direct current

H_C **:** Critical magnetic field

H_{C1} **:** Magnetic field in which it is fully superconducting

H_{C2} **:** Magnetic field where superconductivity starts

J_c **:** Critical currunt density

K **:** Kelvin

SEM **:** Scanning Electron Microscope

T **:** Temperature

T_c **:** Critical Temperature

T_{onset} **:** Critical temperature at which superconductivity starts

T_{offset} **:** Critical temperature where it is fully superconducting

T_p **:** Peak Temperature

XRD **:** *X-Ray Diffractometer*

ACKNOWLEDGEMENTS

The author wishes to express his deepest gratitude to his supervisor **Prof. Dr. Cabir TERZİOĞLU** and **Prof. Dr. Ahmet VARİLCİ** for their guidance, advice, criticism, encouragements and insight throughout the research.

The technical assistance of Doç. Dr. Sevgi POLAT ALTINTAŞ, Prof. Dr. Osman GÖRÜR and Doç. Dr. Sedat ÇETİN are gratefully acknowledged.

and especially to my family

1. INTRODUCTION

Below the specific temperature, the material with no resistivity is called as a superconductor. When the current flows on the superconductors, which has no resistivity, therefore it goes on forever if the temperature is below the critical temperature, T_c. The flowing current should not exceed a specific point in this process. When defining the superconductors, it is not enough to say only zero electrical resistivity exist. Moreover, superconductor materials display perfect diamagnetic properties. Therefore, superconductors repel the magnetic field completely. Superconductivity appears only below T_c, critical current density, J_c, and critical magnetic field H_c. Thus, it is important to get information about three critical parameters, T_c, H_c and J_c, which define the order of superconductivity as shown in Figure 1.1. In addition, as can be seen from the figure, J_c depends on either the function of magnetic field or the function of temperature whereas H_c depends on the function of temperature.

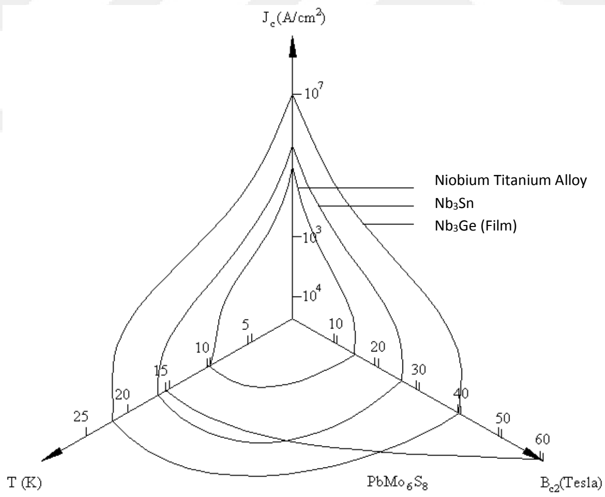

Figure 1.1 *Phase Diagram*

History of the low temperature physics began in 1908 after Heike Kamerlingh Onnes (Holland physicist) liquidized the Helium boiling at 4.2 K. After three years, in 1911, Onnes et. al. discovered the superconductivity phenomenon when investigating the low temperature resistivity for metals at low temperature. They realized that the resistivity dropped sharply to an immeasurably small value at 4.15 K when they investigated the mercury (Figure 1.2). In fact, they won the noble prize in 1913 [1,2].

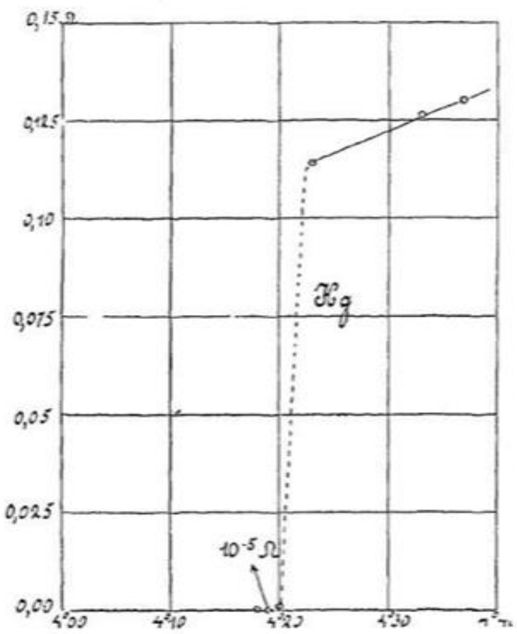

Figure 1.2 *Resistivity goes to zero at T_c*

Above T_c, mercury material has the finite resistivity while the resistivity goes to zero below T_c in which material called as a superconductor.

In 1933, Meissner and Ochsenfeld, German Physicists, investigated the magnetic shielding properties of the superconductors. They analyzed that superconductor cooled under the magnetic field excludes the magnetic flux and does not let the flux penetrate in it as displayed in Figure 1.3. This phenomenon is called Meissner Effect [3].

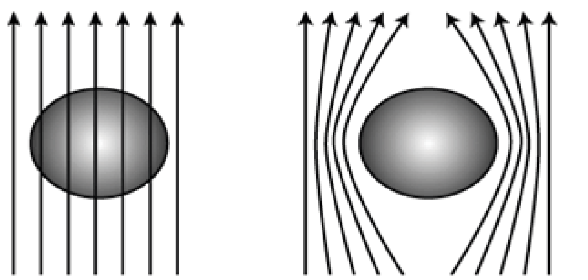

Normal state *Superconductor state*

Figure 1.3 *At $T \leq T_c$, excluding of magnetic field*

In addition, it was observed that superconductivity disappears when external magnetic field exceed the specific H_c value. Namely, superconductivity phase phenomenon is observed below the T_c, J_c and H_c. Superconductor niobium-nitride was discovered at 16 K in 1941 [4]. First theory about superconductivity was established by Cooper, Barden and Schrieffer called BCS theory in 1957. The basis of his theory is explained charge carriers generate opposite momentum electron pairs known as Cooper pairs in superconductors. However, at higher temperatures and with different superconductor systems, the BCS theory has become failed for high temperature cuprate and MgB_2 superconductors [5,6]. Moreover, Alexei Abrikosov found that there are two types of superconductor material named as Type-I and Type-II in 1957 [7]. The Type-I excludes magnetic flux completely from its interior whereas magnetic flux penetrates to Type-II only at small fields, but partially in higher external fields. The Type-II materials can sustain superconductivity in mixed state even higher than 10 T. Therefore, Type-II superconductors are the ones that are of interest for most large-scale applications.

B. Josephson forecasted an unusual phenomenon named weak superconductivity or the Josephson effect in 1962 and it is used for practical applications [8]. A Josephson junction is a structure formed by two superconducting electrodes separated by a thin non-superconducting (tunnel) layer. In figure 1.4, a typical junction is depicted. The electrodes are superconducting plates of width *w*, length *L* and thickness *D*, while the tunnel layer is of thickness *d*. The thin lines show the magnetic field *H*, due to the vortex, which penetrates the electrodes and extends into free space. The extended stray magnetic field creates the additional surface current J_s.

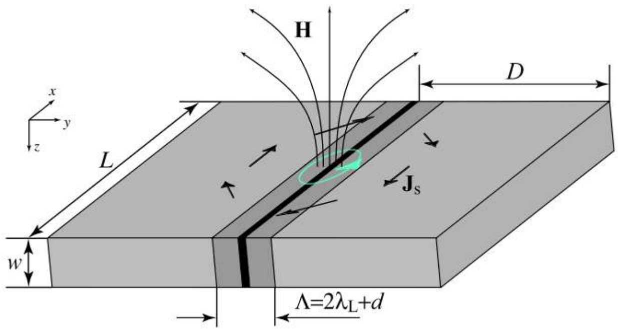

Figure 1.4 *Schematic view of an edge-type long Josephson junction.*

In 1986, J. Georg Bednorz and K. Alex Müller pointed out T_c above 30 K for an oxide of lanthanum, barium and copper. Therefore, research on high temperature superconductivity has started [9].

K. Wu and Paul Chu discovered $Y_1Ba_2Cu_3O_7$ (Y-123) ceramics above liquid nitrogen temperature at T_c = 92 K in 1987 [10]. One year later, Bi (BSCCO) and Tl-cuprate oxides were fabricated at T_c =110 and 125 K, respectively [11,12]. Since then, several research groups have claimed even higher T_c, but they were not reproducible or independently supported by other scientists.

In 2001, it was observed that magnesium diboride (MgB_2) is an extraordinary new superconductor. It is found that the transition temperature of magnesium diboride, does not contain any copper, at 39 K far above the highest T_c of any of the elemental or binary alloy superconductors [13]. While T_c of MgB_2 is still well below that of ceramic superconductors (BSCCO and Y-123), productions of MgB_2 have paved the way for its use in industrial applications. Laboratory testing showed that MgB_2 has more outperformance than that of NbTi and Nb_3Sn wires in magnetic resonance imaging (MRI).

At last, the discovery of high T_c iron and arsenic superconductors (AsFe) were found in 2008 [14]. These compounds do not contain copper but have oxygen, flour or arsenic and iron.

2. SUPERCONDUCTIVITY AND MgB_2

2.1 Superconductor Types

Superconductors can be classified in two types: Soft and hard superconductor. The first type superconductor is composed of metal and metalloids. Although it has some resistance at room temperature, it behaves as superconductor when cooling below the critical temperature. The first type superconductor indicates sharply translation to the superconductor, moreover; it has a perfect diamagnetism property. On the other hand, copper, silver and gold elements, perfect conductors at room temperature, do not behave as superconductor. B_C (H_C) values of some superconductor elements are displayed in Figure 2.1.

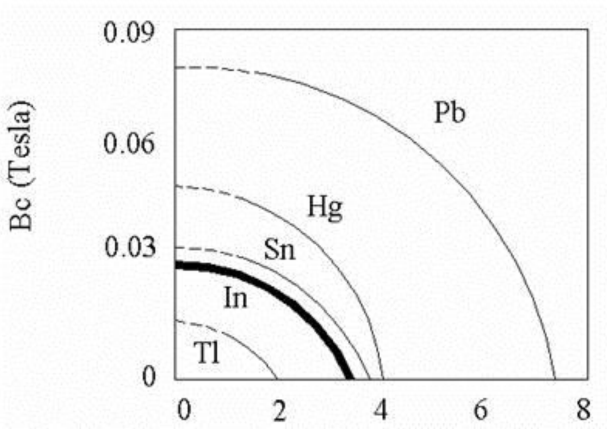

Figure 2.1 *Critical field vs applied field plot for various elements*

As seen from the figure, when magnetic field is about 0.03 T for the Type-I superconductors, superconductivity disappears. Therefore, high magnetic field magnet cannot be produced from these type superconductors. Type-II superconductor is known as 'Hard' superconductor composed of metallic compounds and metallic mixtures except for vanadium, technetium and niobium. T_c of these type superconductors is quite higher than that of the Type-I superconductors while they behave as superconductor at liquid nitrogenous temperature instead of liquid helium. Unlike the Type-I superconductor, even though they have no sharply translation to the superconductor, it can be mentioned from the specific mixed state. The Type-II start to behave as superconductor before attaining in the mixed state (Figure 2.2).

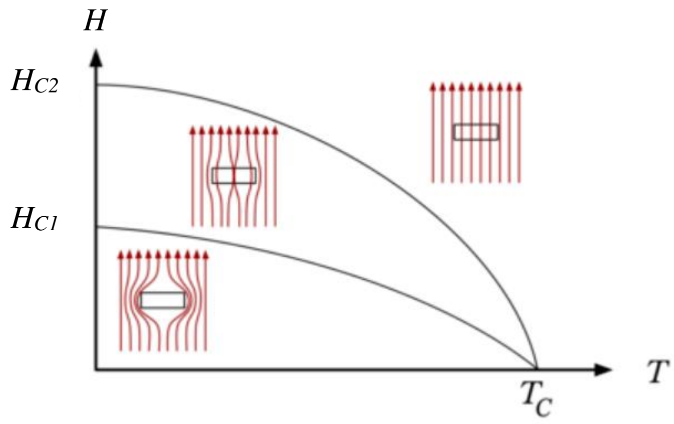

Figure 2.2 *Temperature versus magnetic field behavior of Type-II superconductors*

Here there is an interesting point: normally there are many ceramics used as insulators; however, they are used as high temperature superconductor now. By 1950, the Type-II superconductors were investigated. Superconductivity translation point of these type materials can be determined by two critical fields as H_{C1} and H_{C2}. The Type-II material is an exact superconductor under H_{C1} field whereas the vortexes are formed between H_{C1} and H_{C2}, (Figure 2.2). Therefore, they are in the mixed state at which external magnetic field penetrates to the material. When the external field exceeds H_{C2} field value, the material loses totally superconductivity property.

Table 2.1 *Variation of T_c for Type II Superconductors.*

Element	T_c (K)	H_{C2} (0) (T)
Nb_3Al	*18.7*	*32.4*
Nb_3Sn	*18.0*	*24.5*
Nb_3Ge	*23*	*38*

As seen from Table 2.1, H_{C2} (T) values are larger than H_C values of the Type-I superconductors. Thus, the Type-II superconductors are useful for magnets to generate the high magnetic field. Figure 2.3 shows change of internal magnetic field with the external magnetic field for the first and second type superconductor at the constant temperature.

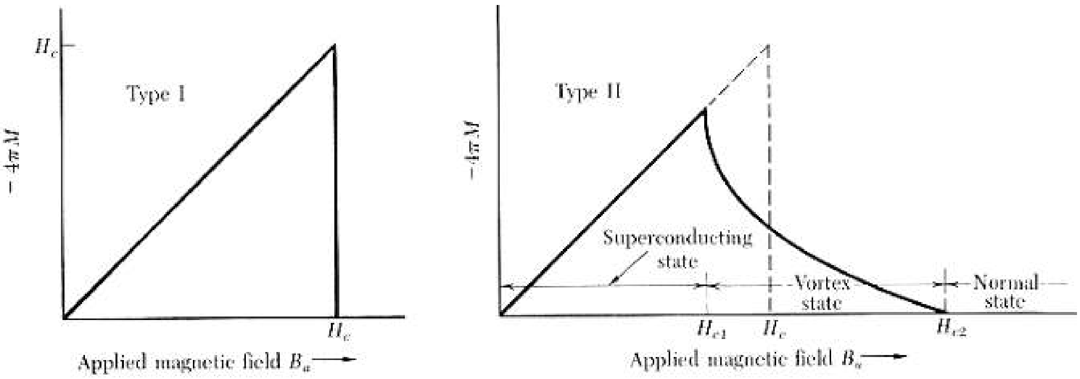

Figure 2.3 *Magnetic behavior of the superconductor.*

Penetration depth and coherence length are very important parameters in order to study superconductors. Penetration depth in superconductors is defined as a measure of length that the applied magnetic field can penetrate a material. For Type-I superconductors, the relationship between magnetic field and penetration depth, λ, can be given as

$$B(x) = B_0 e^{-x/\lambda}$$

where λ and B_0 are the penetration depth and value of the magnetic field at the surface, respectively. The graph of variation of the magnetic field inside a Type I superconductor with distance is depicted in Figure 2.4. The typical value of the λ is in the range of 10–100 nm. The relationship between penetration depth and temperature can be written as

$$\lambda(T) = \lambda_0 [1 - (T / T_c)^2]^{-1/2}$$

where λ_0 is the penetration depth at T = 0 K [15].

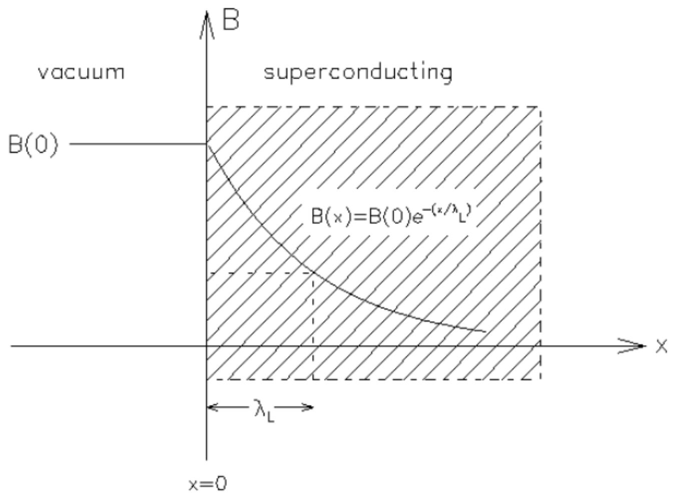

Figure 2.4 *Schematic decay of magnetic field in the interior of a superconductor*

Definition of the coherence length, ξ, for superconductors can be defined as the maximum distance that electrons of a cooper-pair is correlated. Both ξ and λ deviate at T=T_c. The relationship between them, Ginzburg–Landau parameter, k,

$$k = \lambda/\xi,$$

stay finite as $T \rightarrow T_c$. The value of k gives information about the types of superconductor: k << 1 (i.e. λ << ξ) for Type-I superconductors and k >> 1 (i.e. λ >> ξ) for the Type-II [16].

2.2 Magnesium Diboride - MgB_2

MgB_2, known for half century, is a compound used in the science and industrial world, and is especially used in the area to be held high magnetic field. Akimitsu et al presented research [13] in 2001. Therefore, it was understood that MgB_2 is superconductor at 39 K (Figure 2.5) and has a perovskite structure as shown in Figure 2.6.

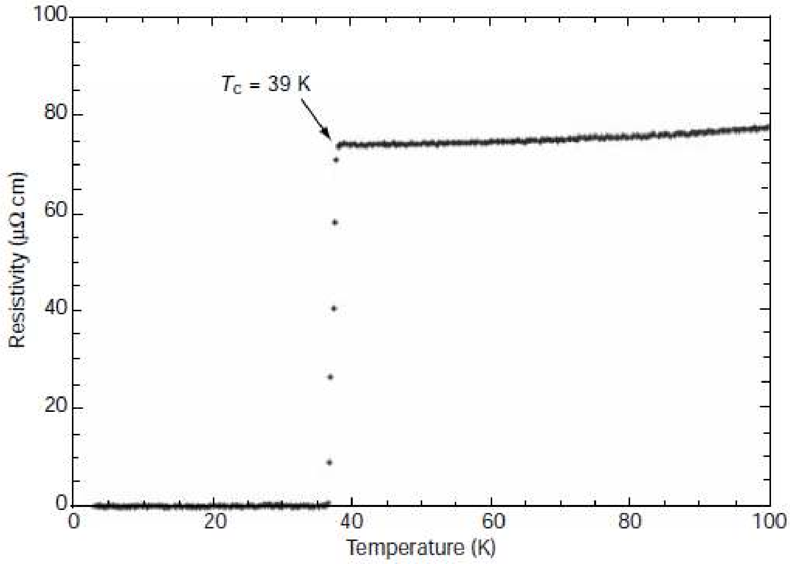

Figure 2.5 *Resistivity versus temperature graph for MgB_2*

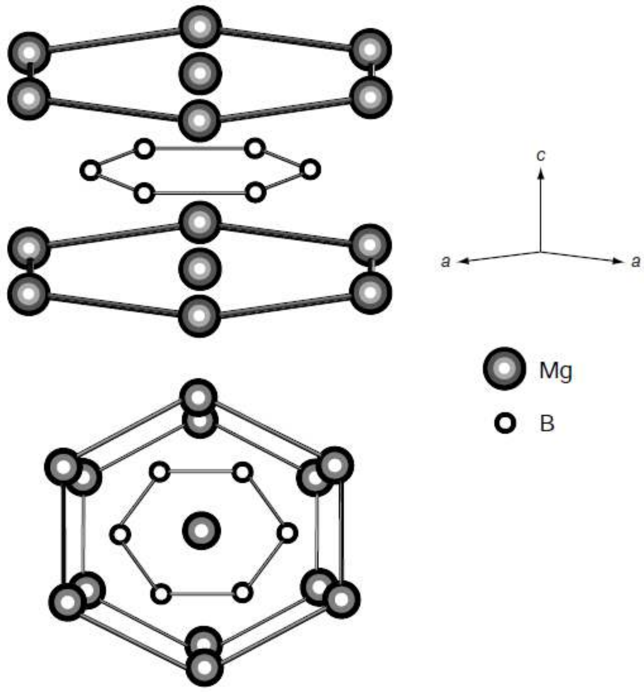

Figure 2.6 *Crystal structure of MgB_2*

This investigation started the intense study field in the world. The first important reason of intense interest is that MgB_2 is a metallic superconductor appears at 39 K which is high critical temperature. Secondly, because Boron atom is superconductor, so it comes up with the test about prediction of the BCS theory by investigating the isotope effect. After investigation of the MgB_2 superconductor, works on the boron atom proved isotope effect. Boron isotope effect and band structure studies points out the connection between electron and phonon coupling of superconductivity in this compound. Measurements of the H_c and J_c proved the Type-II superconductor for MgB_2. Thirdly, maybe the most important reason is that the MgB_2 superconductor compound has more stable state, so it is useful for technology. Critical temperature (39 K) of MgB_2 is higher than the T_c of metallic superconductors while it is lower than the critical temperature of the Cu-O compound superconductors discovered in 1986. Therefore, it can be thought as restrictive factor in technology. However, development on the cooling "crycooler" technology in last decade has shown that MgB_2 uses micro-electric and machine in the technology fields. In addition, intensive works on fabrication of thin film MgB_2 has been continued [17]. There are two main properties for any superconductor material. The first one of them is that the resistivity of material goes to zero when cooling the below the specific T_c value. The second of them is that they behave as perfect diamagnet below this critical temperature and low enough magnetic field. After the fabrication of superconductor, for the characterization of the superconductor, either by using resistivity measurements the electrical properties are determined or by using magnetic measurements without contact with superconductor magnetic properties are determined. AC susceptibility is the best method to determine the magnetic properties of the superconductors. AC susceptibility is a relation between peak and zero-point values of applied magnetic field or magnetization appearing when magnetic flux goes inside the sample. The most important property is to separate a signal relation with magnetization as in-phase (χ') and out of phase (χ'') as harmonic susceptibility and allow to take easily measurements. Phase adjusting is important for accuracy of experiment results.

MgB_2 well characterized is a component in hexagonal crystal structure (Fig. 2.6.). As well-known from literature, it is in AlB_2 structure. Research has become interesting since the superconductor structure of MgB_2 is discovered in 2001. Intergranular weak links of MgB_2 are problem for ceramic high temperature superconductor, unlike that; they behave as different for MgB_2 superconductor and so J_c which appears at the boundaries can be compared with intergranular J_c. However, unlike the high temperature superconductor, MgB_2 translates the normal state lower critical magnetic field. For this reason, application area for MgB_2 is restricted. It has the similar properties with Nb_3Sn compound used widespread for superconductor applications. MgB_2 is interesting and useful material for technology thanks to higher transition temperature, lower density, either Mg or B atoms are abundant. Stoichiometric amount of Mg and B powders reacting with each other nearly 2 hours at 950^0C to fabricate the MgB_2 powder which is commercial material owing to chemical applications.

As well as electrical properties, mechanic properties and cost are useful to use widespread a superconductor material. Magnesium diboride with 39 K transition temperature as some high temperature superconductors does not work in the liquid nitrogenous environment, however; nowadays closed-circuit cooling system is widespread and makes the temperature go down nearly 2 K. Furthermore, when it is in normal state about 40 K, the resistivity is below 0.5 μΩ cm (but it can be changed with fabrication method) which are desirable properties. On the other hand, transition state of Nb_3Sn appears at 20 K where the resistivity is 11 μΩ. At the room temperature the resistivity is 9.6 μΩ for MgB_2 and 80μΩ for Nb_3Sn, respectively. Thus, resistivity is in favor of MgB_2. On the other hand, critical current level of MgB_2 is lower than that of Nb compound superconductors. Provided this value, however, increases density of the material, it is expected that the value can be increased by decreasing distance of intergranular and by forming magnetic flux pinning centers. On the other hands, like the copper oxide superconductors, the results of performance adjustment are inefficiency via the displacement of the chemical material. Al atom doped instead of Mg atom causes to disappear completely the superconductivity.

Many various methods have been tried to show MgB_2 is useful to fabricate the thin cable, filament, etc. and good enough results have been taken. The materials are still fragile. Most important part of the research deals with solving this problem. For the cost of MgB_2 as a material which is cheaper than fabricated by Nb material. However, the final fabrication cost will be determined by means of the method including the process of raw metal.

3. MATERIALS AND METHODS

3.1 Preparation of The MgB_2 Samples

A commercially available MgB_2 powder (Alpha Aesar) was used as the starting material for the preparation of MgB_2 superconducting samples. In order to fabricate the pellet samples, the starting powder was pressed in rectangular shape (with surface area of 4x10 mm^2 and thickness of 1 mm) under 100 MPa pressure as shown in Picture 3.1. The pellets in this state are not superconducting. In order to produce MgB_2 superconducting samples, a heat treatment called annealing was chosen to be 650, 750, 850 and 950°C in flowing Ar gas for preventing oxidation for 2 h. The annealing processes was carried out in the high temperature resistant quartz tube that inserted inside the three-section tube type furnace (Picture 3.2). In order to reduce the interaction between the sample and the quartz tube in the furnace during heat treatments after the sample is placed in the middle of the furnace, and to minimize the effect of any residual O_2, the samples were wrapped with Ta foil since Ta is well known to be a very efficient O_2 acceptor. In the annealing procedure under Ar flowing, it was heated to the selected temperatures (650, 750, 850 and 950°C with a scan speed of 6°C per minute, and after waiting at these temperatures for 2 hours, the oven was turned off and let it cool to room temperature. After the heat treatments, the four different MgB_2 superconductor samples were obtained with different annealing temperature. After the time being, the samples annealed at 650, 750, 850 and 950^0C in 2 hours in Ar atmosphere were called as S650, S750, S850 and S950.

Picture 3.1 *TÜMAS press machine and mold*

Picture 3.2 *Quartz tube and PROTHERM programmable tube furnace*

3.2 XRD Measurements

A diffractometer is a device that uses a beam of radiation or particles (such as X-rays or neutrons) to analyze the structure of a material, displaying the pattern of rays scattered from the material. In this thesis, a Rigaku D/Max-IIIC Jeol Multiflex diffractometer (Picture 3.3) was used with Cu-Kα radiation (λ= 1.5418 Å) in the range of 2Θ = 3°- 60° at room temperature with a 0.02° step increment and a scanning speed of 3°/min. beam diffraction (XRD) data were obtained. XRD measurements give about lattice parameters, average crystalline size and phase purity for the produced samples.

Picture 3.3 *Rigaku X-Ray Diffractometer*

3.3 SEM Measurements

The Scanning Electron Microscope (SEM) is a type of electron microscope that views the surface of the sample using a high-energy electron beam with a raster scanning pattern. A result signal is produced as electrons interact with the atoms of the sample. The signals contain information about the properties of the samples such as surface topography, composition and electrical conductivity. The surface morphology of the superconducting samples was examined with a JEOL JSM-6390LV SEM as displayed in Picture 3.4.

Picture 3.4 *JEOL JSM-6390LV Scanning Electron Microscope.*

3.4. Resistivity Measurements (R-T)

In order to study the electrical properties of a superconductor (characterization process), we performed resistivity as a function of temperature at 0.0, 0.5, 1.0, 2.0, 3.0, 4.0 and 5.0 T measurements by using the four probe method (four wires attached to the rectangular shaped samples with silver paint, two outer wires for current and two inner wires for voltage). In order to measure the resistance of the sample, a current (5 mA) is passed through the sample and the voltage (potential difference) is recorded momentarily. The resistance were obtained from the $R = V/I$ (Ohm's law). These measurements were carried out in He gas cooled Cryostat device that can operate between 10K-300K (Picture 3.5). The sample was glued to the cold head part of this device with wax that provides therm al conductivity as displayed in Picture 3.6.

As known, the superconducting materials are superconductor (zero resistivity) below a certain temperature called the critical transition temperature, T_c Since the transition temperature of MgB_2 is around 39 K, it was decided to measure the resistivity between 15 and 50K. Thus, the critical temperature values (T_c) of the samples were determined with zero resistance. In the measurements, the average of the measured value was taken by applying +5mA and –5mA current to the outer ends of the samples, respectively. Figure 3.1

Picture 3.5 *He gas cooled cryostat*

Picture 3.6 *Sample mounting on the cold head*

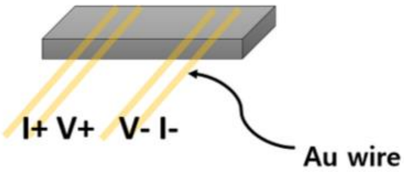

Figure 3.1 *Contacts of samples*

3.5. R-H Measurements

For the R-H measurements, He gas cooled Cryostat device was also used. The difference between the R-T and R-H measurements is the resistivity as a function of temperature at a constant magnetic field for R-T measurements while the resistivity as a function of applied magnetic fields at a constant temperature. After the samples were first cooled to below T_c, the temperature was kept constant and the magnetic field was swept from zero to the value where the superconductivity was broken, and then the critical magnetic field values at this temperature were recorded (Picture 3.7).

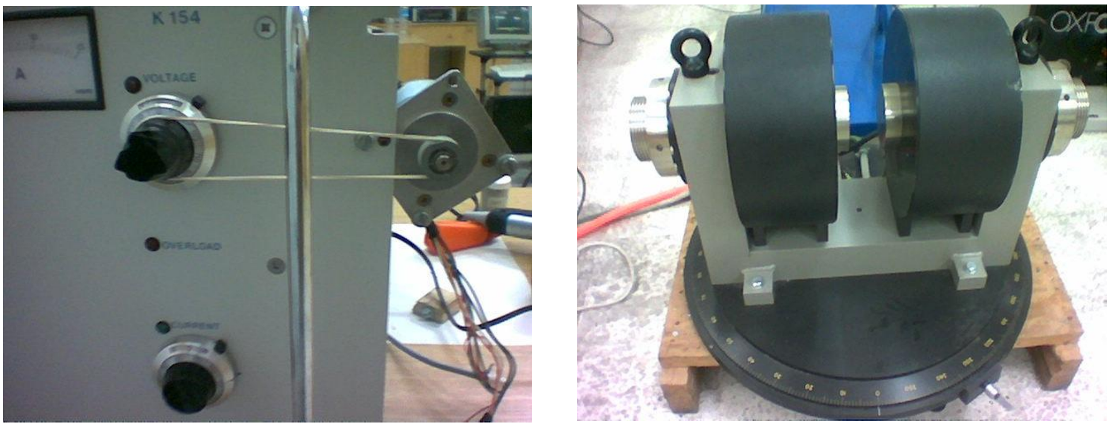

Picture 3.7 *DC Magnet System*

3.6. AC Susceptibility Measurements

AC Susceptibility measurements were carried out in the cryostat with the help of Hall Generator in a homemade setup. In this setup, a 63.3 mm long and 20 mm diameter coil with 1266 windings (Picture 3.8), which creates an external magnetic field with the driver voltage, was placed to include the cold head of the cryostat, the sample and the hall generator. When the sample was placed in the cold part of the cryostat (Figure 3.2), because the samples did not reach the desired position in the coil, so it was ensured that the sample came to the appropriate place in the coil with a quartz glass piece which has a very good thermal conductor (Picture 3.9). A Si diode attached to the cold head was used to measure the temperature, as the sample did not touch the head of the cryostat. The temperature reading accuracy of this Si diode was around 20 mK. Then, the Axial Hall generator from Lakeshore Company with 0.55 mV / kG magnetic sensitivity and 0.08 cm diameter active area was placed on it touching the sample (Picture 3.10). A control current of 200 mA was applied to the Hall generator. As the applied magnetic field to the outer coil wound by hand was excluded by the superconductor, the susceptibility signals of the Hall generator magnet were captured with a Lock-in amplifier and recorded using a Labview computer program. The measurements were made at AC field of 240, 480, 720, 960 and 1200 A/m at a frequency of 10 Hz. After the samples were first cooled to around 15 K and kept at this temperature for a while (the sample was expected to reach thermal equilibrium), measurement data were taken with a heating rate of 0.5 K / min in the temperature range of 30 to

45 K. Since the signal produced by the Hall generator is very weak, a Tegam model 73 precision ratio converter was used for a voltage amplifier.

Susceptibility signals consist of 3 harmonics. With this mechanism, we measured the 1st harmonic signal of susceptibility. The Lock-in amplifier separates the only signal from the sample into two parts; real and imaginer parts of the signal.These measurements were plotted and then the susceptibility-temperature curves were obtained. The peak point (peak point) of the curve in the imaginer part gives the peak temperature, T_p, J_c^{-inter} (critical current density between particles) values were calculated with the Bean's model depending on the applied area and the thickness of the sample. Since the thickness of the sample and the applied area were equal, J_c^{-inter} was equal for all samples. However, these critical current values are at different peak temperatures for each sample. T_{onset} and T_{offset} values were found from the real part of the graphs. [18-21]

Picture 3.8 *AC Susceptibility measurements coil*

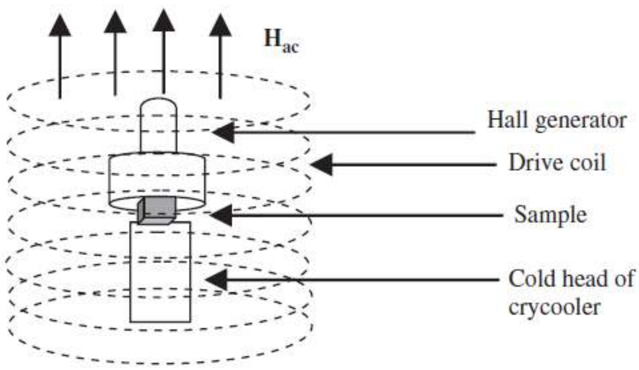

Figure 3.2 *Homemade Hall probe AC-Susceptibility measurement system*

Picture 3.9 *The quartz glass piece*

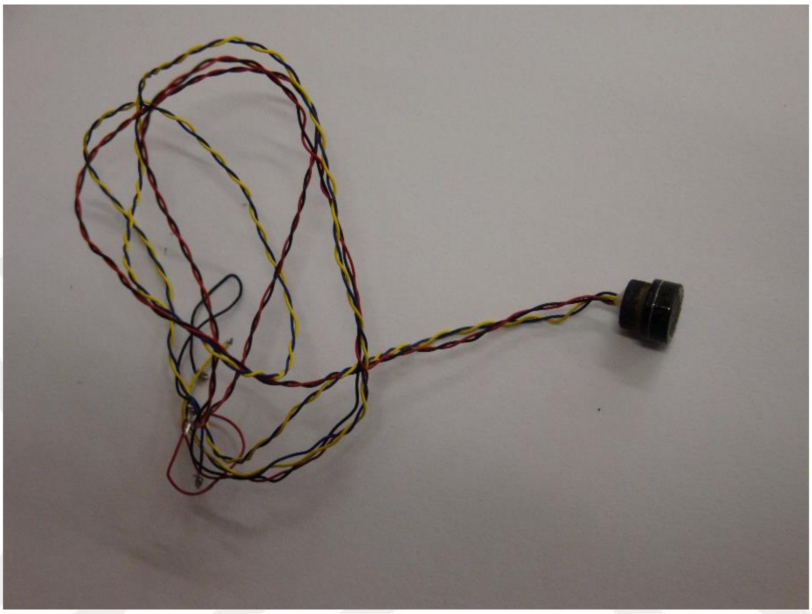

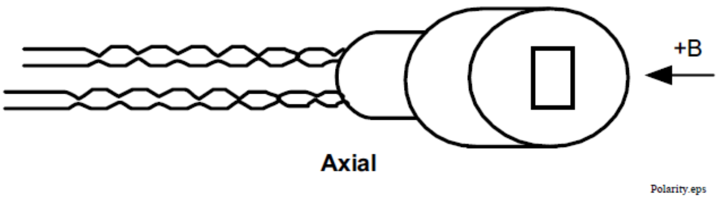

Picture 3.10 *The Axial Hall generator*

4. RESULTS AND DISCUSSION

MgB_2 has a high T_c of 39 K and can operate in the 20-30 K temperature range with cryocoolers where low temperature superconductors cannot be used. For this reason, the cost of making usable materials of MgB_2 is lower than the most commonly used NbTi and Nb3Sn. The superconducting properties of MgB_2 have shown that it has already achieved or even exceeded many of the critical properties of low-temperature superconductors. On the other hand, it has been seen that the engineering current density of MgB_2 wires with superconducting materials used in practice is at applicable levels. MgB_2 has weak unbound grain boundaries and grain boundaries serve as good pinning centers [22-27]. Long multifilament forms of MgB_2 are easy to prepare and raw materials are inexpensive. The density of MgB_2 is much lower than other superconductors and therefore suitable for light applications. MgB_2 can be configured in round and rectangular cross sections, providing flexibility in coil design and fabrication. MgB_2 can be prepared using a number of inexpensive and readily available sheath materials, and the process only requires a lower heat treatment temperature and time. From an industrial point of view, these are significant advantages and therefore MgB_2 is considered the material for the next generation of high field magnets [28,29]. MgB_2, which can be made a better superconductor with the effect of fabrication parameters, will become more useful industrially. In this thesis, the effects of annealing temperatures on the microstructure, electrical and magnetic properties of superconducting samples of MgB_2 were studied by performing XRD, SEM, R-T, R-H and AC susceptibility as a function of temperature experiments.

4.1 XRD Analysis

XRD measurements were made by using an XRD (Jeol Multiflex) at room temperature. The lattice parameters (*a* and *c*) of the crystal structure were extracted from these XRD peaks.

Some of the Miller indices are depicted for all the samples in Figure 4.1. As can be clearly seen from the XRD patterns of the sample S950 that the presence of minor elemental Bor (B) peaks were observed as well as MgB_2 while there were no traces of MgO, MgB_6 or MgB_{12}. However, in comparison with the other samples

(S650, S750 and S850), these B peaks were not detected [30,31]. This result indicates that the annealing temperature 950 ^{0}C is too high for the samples of MgB_2 and may cause the separation of elemental B through its sublimation. Moreover, no traces of MgO peaks were observed for the samples S650, S750 and S850 in the XRD patterns due to the use of argon gas during the annealing of the samples prevented the oxidation of Mg. As the annealing temperatures increased from 650 to 850°C, the values of 2Θ at maximum peak shifted to smaller angles and the intensity of all the peaks (the full-width and half maximum) increased (decreased) while they shifted to higher angles and the intensity of peaks (the FWHM) decreased (increased) at 950°C. The all the MgB_2 samples annealed at different temperatures showed polycrystalline structure. The increment in the intensity of the peaks indicates an increase in the size of the crystal as will be confirmed in the SEM analysis.

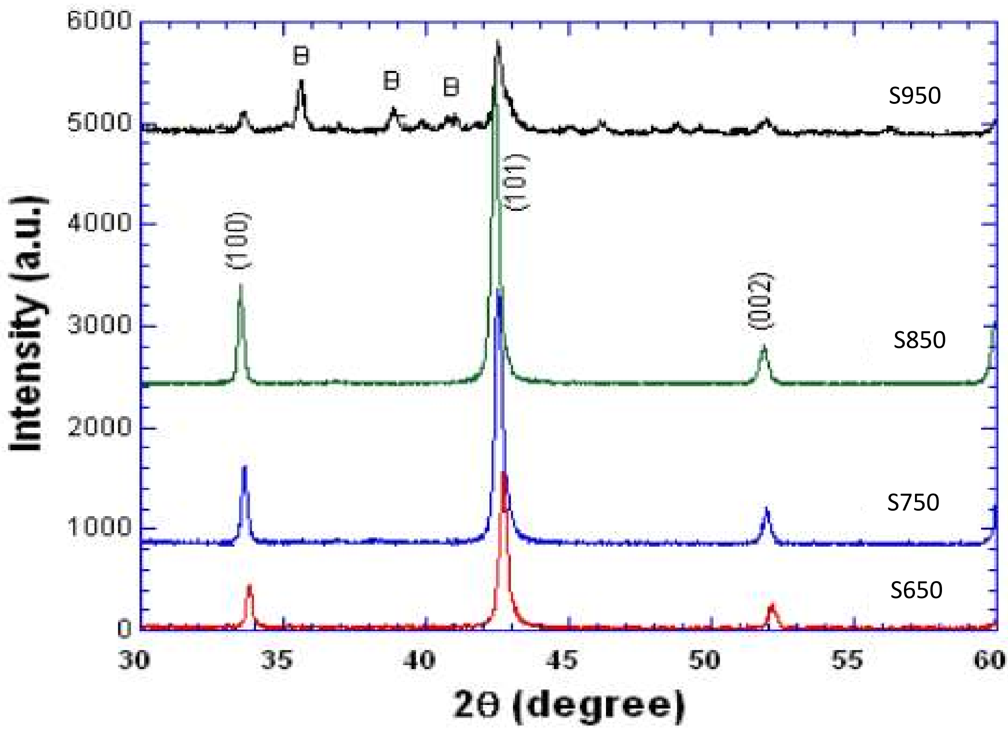

Figure 4.1 *XRD patterns for the S650, S750, S850 and S950 samples*

Lattice parameters *a* and *c* were extracted with the Least-Square Fits method. The calculated lattice parameters *a* and *c* extracted from the (100) and (00l) peaks of the XRD patterns are listed in Table 4.1. The in-plane B-B distance proportional to the lattice parameter *a* while the interplanetary B-B distance proportional to the lattice parameter *c* [30-34]. The crystallographic symmetry of the material is hexagonal and the unit cell parameters (i.e., *a* and *c*) are found to be 3.0701 and 3.2522 Å for the sample S650, 3.0723 and 3.3522 Å for the sample S750, 3.0844 and 3.5285 Å for the sample S850, and 3.0752 and 3.5090 Å for the sample S950, respectively. A noticeable change in the lattice parameters of the samples was obtained within the experimental limit of 0.0001 Å. From these results, we can conclude that the parameter *a* increased slightly from 3.0701 to 3.0844 Å and the parameter *c* increased significantly from 3.2522 to 3.5285 Å with the increase in the annealing temperature from 650 to 850°C while the parameters a and c increased which are reasonably consistent with the other studied [35].

Table 4.1 *The lattice parameters a and c for all the samples and density of samples*

Samples	***a* (Å)**	***c* (Å)**	***Density (g/cm^3)***
S650	3,0701	3,2522	1.922
S750	3,0723	3,3522	1.950
S850	3,0844	3,5285	2.180
S950	3,0752	3,5090	2.002

The calculated crystallite size from the XRD peaks using Scherrer–Warren equation from the full-width and half maximum (FWHM) was found to be between 50-70 nm for S650, S750 and S950 samples while it was 100 nm for the sample S850. The decrement (increment) in the FWHM (the intensity of the peaks) with the increase in the annealing temperature from 650 to 850 °C reveals that crystallite size increased as confirmed by the SEM analysis.

4.2 SEM Analysis

In order to study the surface morphology and microstructure for the samples, SEM measurements were performed using the JEOL 6390-LV instrument. The surface micrographs for all the samples annealed are depicted in Figure 4.2. The extracted grain sizes using program was found to be about 100-120 nm for both the samples S850 and S950 while more traces of partial melting because of high heat treatment temperature was observed for the sample S950. Mg sublimation at the grain boundaries and separated boron accumulation were seen in the micrograph for the sample S950 which reveals the existing of B peaks in the XRD patterns. This result will be confirmed by the AC susceptibility as a function of temperature measurements.

However, it was obtained that the grain size of the samples S650 and S750 is smaller than that of the sample S850. These values agree with crystallite size extracted using Scherrer-Warren equation from XRD patterns. As can be seen from Picture 4.1, a better grain connectivity, a denser surface and a decrement in the number and size of voids were observed with the increase in the annealing temperature which is consistent with J_c values of the samples [32,33,36]. It was also obtained that the samples annealed at lower temperature were randomly oriented with a non-uniform surface. It can be concluded from this result that the grain connectivity was poor or weak. It can be also concluded that the lower heat treatment decreased the reactivity for the formation of MgB_2 phase and the best optimum annealing temperature for the MgB_2 samples is 850°C among the samples.

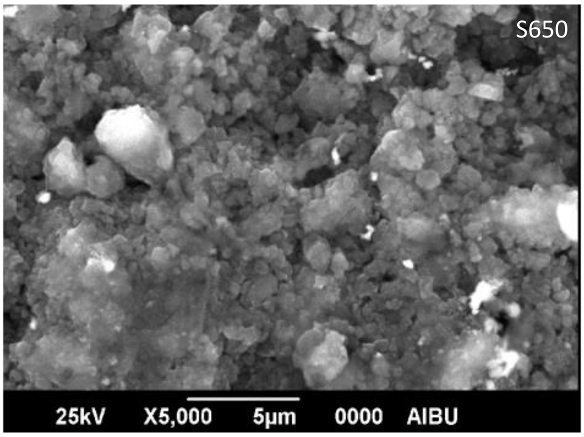

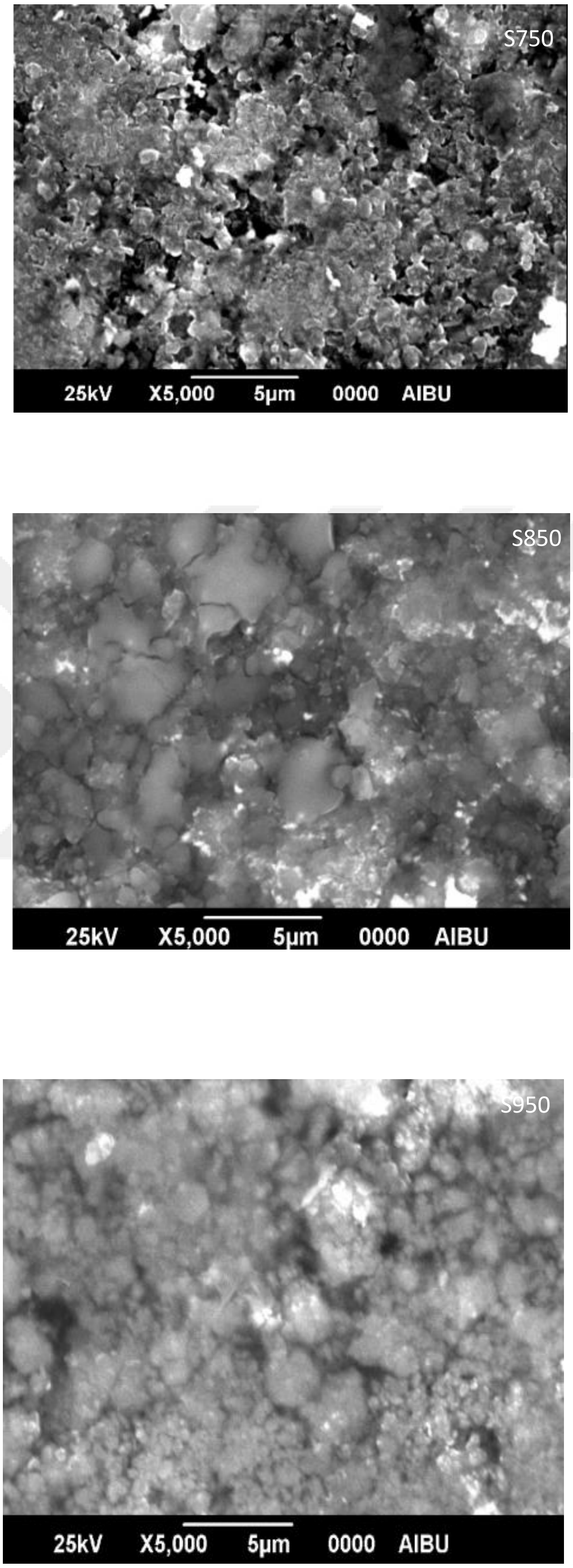

Picture 4.1 *The surface micrographs for all the samples*

The decrease in grain sizes and their orientations worsened coupling between superconducting grains may also be reason of the decreased number of flux pinning centers and of T_c of the samples as will be confirmed by the AC susceptibility and resistivity measurements, respectively.

4.3 The Analysis of Resistance versus Temperature Measurements

Magnetoresistance measurements as function of temperature at 0, 0.5, 1, 2, 3, 4 and 5 T were performed using four-points method for all the samples and displayed in Fig. 4.2. In these measurements, measurements were taken by changing the temperature under a constant external magnetic field.

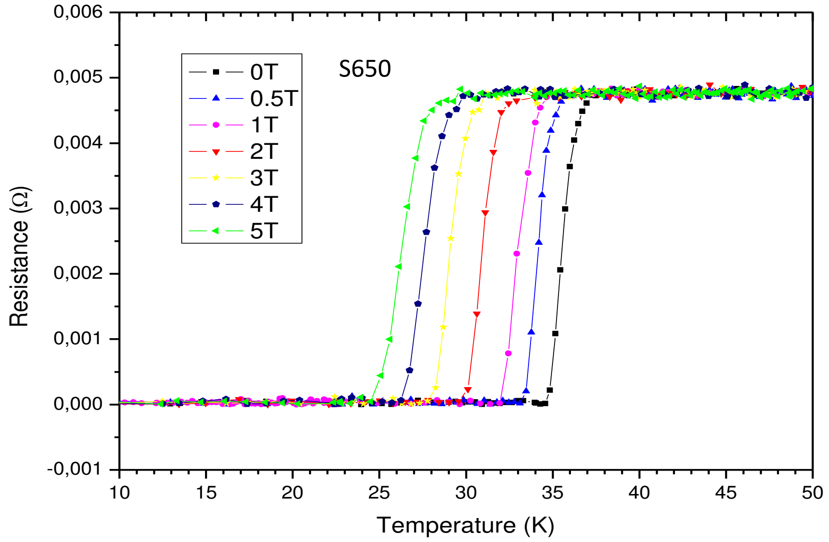

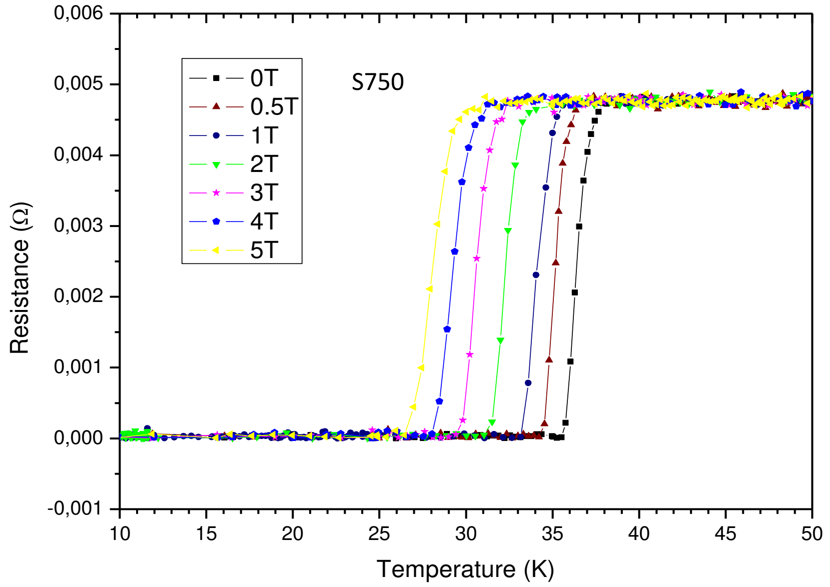

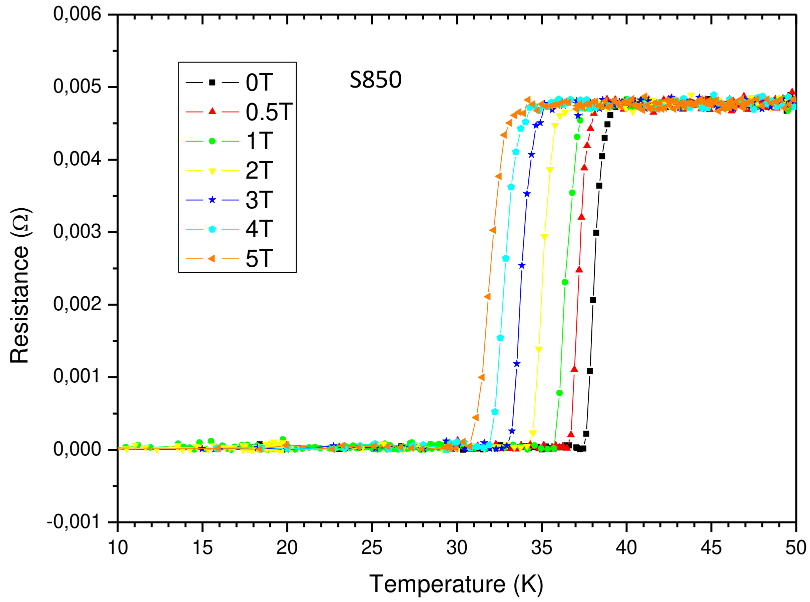

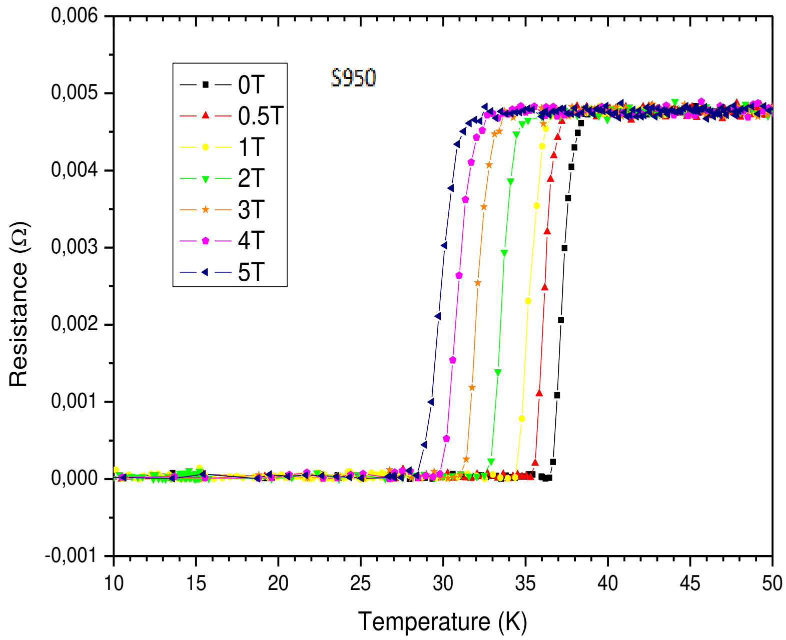

***Figure 4.2** Magnetoresistance versus temperature graph of the samples annealed.*

From the findings of these measurements, the transition temperature values (T_{onset} and T_{offset}) as a function of annealing temperature and applied magnetic field are listed in Table 4.2, graphs AA and graphs BB. As can be seen from the table and graphs, the T_{onset} value increased from 38.1 to 39.6 K while the heat treatment temperature increased from 650 to 850 OC, while it decreased with the increase of the magnetic field, it decreased to 39 K for the S950 sample. It was deduced that T_{onset} also decreased with increasing the magnetic field while it does not change for Bi-2223, Bi-2212 and Y-123 superconductors. The resistance in the normal state increased as the temperature is raised, that is, it shows the metal-like behavior. As a conclusion, T_{onset} value is proportional to the increase in heat treatment temperature while it is inversely proportional to the applied magnetic field. On the other hand, the ΔT temperature transition interval between T_{onset} and T_{offset} temperatures is approximately 3K in the S650, S750 and S950 samples, while this value is approximately 2K in the S850 sample. This shows that the S850 sample is better.

Table 4.2 *The values of transition temperatures* (T_{onset} and T_{offset}) *at 0, 0.5, 1, 2, 3, 4 and 5 T for the samples*

Samples	***S650***		***S750***		***S850***		***S950***	
H_{App} (T)	T_{offset} (K)	T_{onset} (K)	T_{offset} (K)	T_{onset} (K)	T_{offset} (K)	T_{onset} (K)	T_{offset} (K)	T_{onset} (K)
0	***34.7***	***38.1***	***35.6***	***38.7***	***37.7***	***39.6***	***36.6***	***39.0***
0.5	***33.2***	***36.5***	***34.1***	***37.0***	***36.5***	***38.7***	***35.2***	***37.9***
1	***31.9***	***35.6***	***33.2***	***35.9***	***35.8***	***37.8***	***34.2***	***36.9***
2	***29.7***	***33.9***	***31.3***	***34.4***	***34.1***	***36.8***	***32.6***	***35.5***
3	***27.6***	***31.6***	***29.1***	***32.6***	***32.9***	***35.5***	***31.0***	***34.2***
4	***26.1***	***29.9***	***28.0***	***31.7***	***31.8***	***34.6***	***29.8***	***33.0***
5	***24.4***	***29.3***	***26.3***	***30.5***	***30.8***	***33.5***	***28.2***	***31.8***

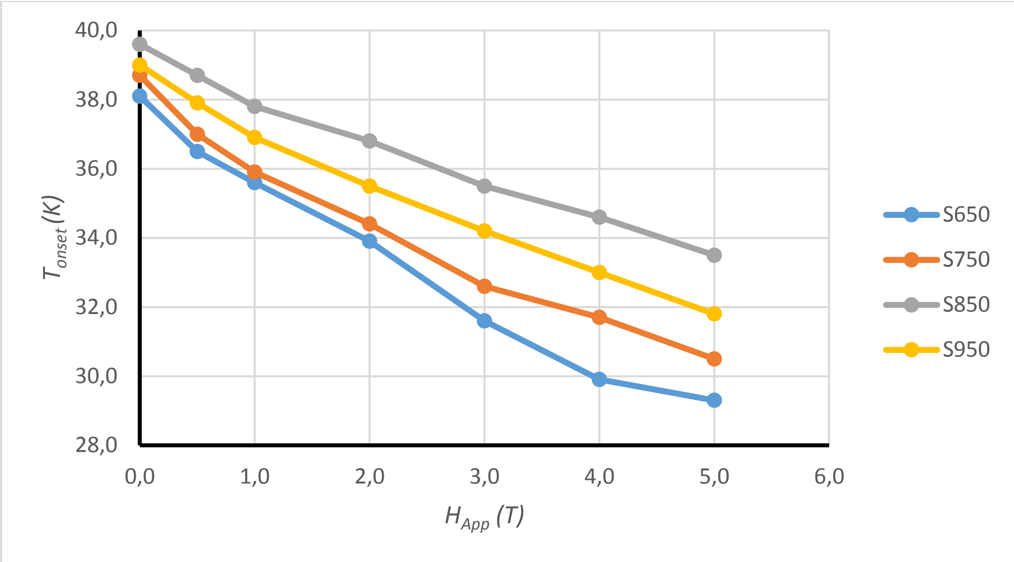

Figure 4.3 *Applied magnetic field versus T_{onset} temperature graph of the samples*

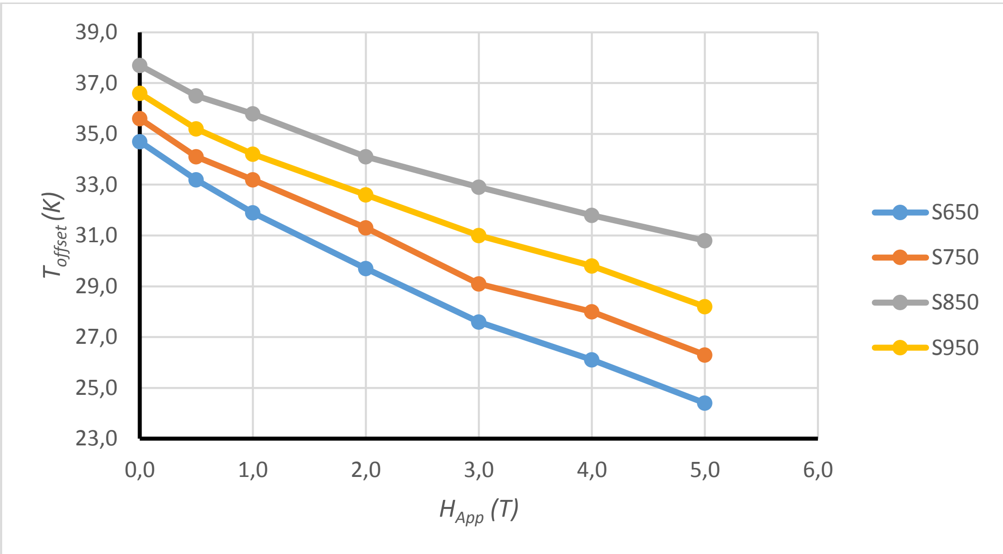

Figure 4.4 *Applied magnetic field versus T_{offset} temperature graph of the samples*

Again, from the findings of the same measurements, the values of the critical magnetic field H_{C2} where superconductivity starts as a function of annealing temperature and temperature and the values of the magnetic field H_{C1} where it is completely superconducting are listed in Table 4.3. As can be seen from the table, when we look at each sample for the same value in the H_{c1} magnetic fields that we apply externally to disrupt the superconductivity; As the heat treatment temperature increases, we see that the superconductivity begins to deteriorate at higher temperatures and decreases again after the S850 sample. This shows us that the

850°C annealed sample is more resistant to the external magnetic field that tries to disrupt the superconductivity. H_{C2} completely behaves in the same way in the transition magnetic fields to superconductivity.

***Table 4.3** The values of temperature at 0, 0.5, 1, 2, 3, 4 and 5 T H_{C1} and H_{C2} magnetic fields for the samples*

S650		S750		S850		S950	
T (K)	H_{C2} (T)	T (K)	H_{C2} (T)	T (K)	H_{C2} (T)	T (K)	H_{C2} (T)
36.7	0	37.2	0	38.7	0	38.0	0
35.0	0.5	35.9	0.5	37.8	0.5	36.9	0.5
34.0	1	35.0	1	37.0	1	36.0	1
31.9	2	33.1	2	35.7	2	34.4	2
30.2	3	31.6	3	34.5	3	33.0	3
28.8	4	30.4	4	33.6	4	31.9	4
27.5	5	29.2	5	32.8	5	30.8	5
S650		S750		S850		S950	
T (K)	H_{C1} (T)	T (K)	H_{C1} (T)	T (K)	H_{C1} (T)	T (K)	H_{C1} (T)
35.0	0	36.0	0	37.7	0	36.8	0
33.7	0.5	34.8	0.5	36.8	0.5	35.8	0.5
32.4	1	33.6	1	35.9	1	34.8	1
30.3	2	31.7	2	34.5	2	33.2	2
28.5	3	30.0	3	33.3	3	31.6	3
26.9	4	38.6	4	32.1	4	30.3	4
25.4	5	27.3	5	31.1	5	28.1	5

4.4 The Analysis of Resistance versus Magnetic Field Measurements

Figure 4.3 depicts the resistance as a function of applied magnetic field for four different temperatures. In these measurements, measurements were taken by changing the magnetic field under the external magnetic field, keeping the temperature constant. From these measurements, we have determined the critical applied magnetic field values, H_{C2}, for different constant temperatures as tabulated in Table 4.4. The H_{C2} value decreased with the increase in the temperature measured for all the samples was clearly observed. In these measurements, there is no way to compare the H_{C2} values with each other because the constant temperature is different for each sample.

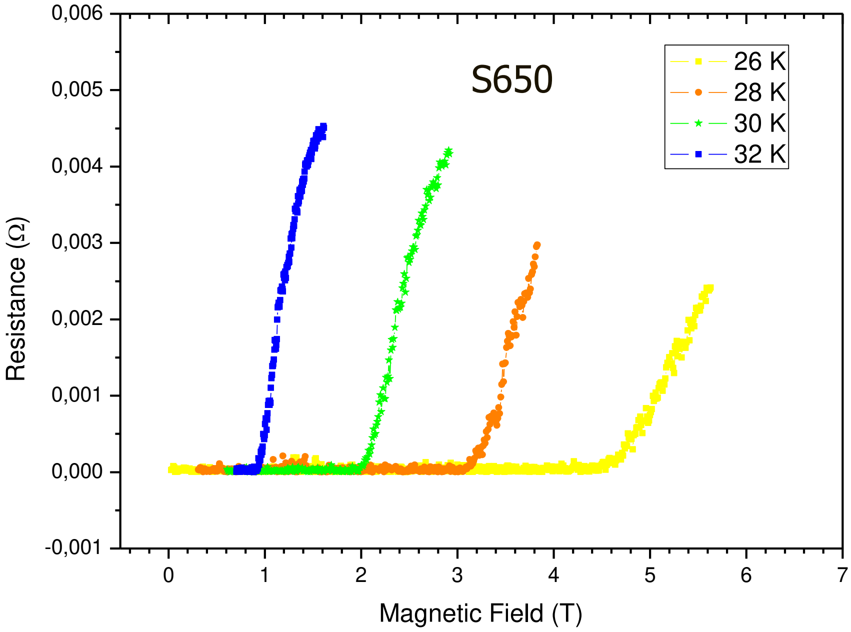

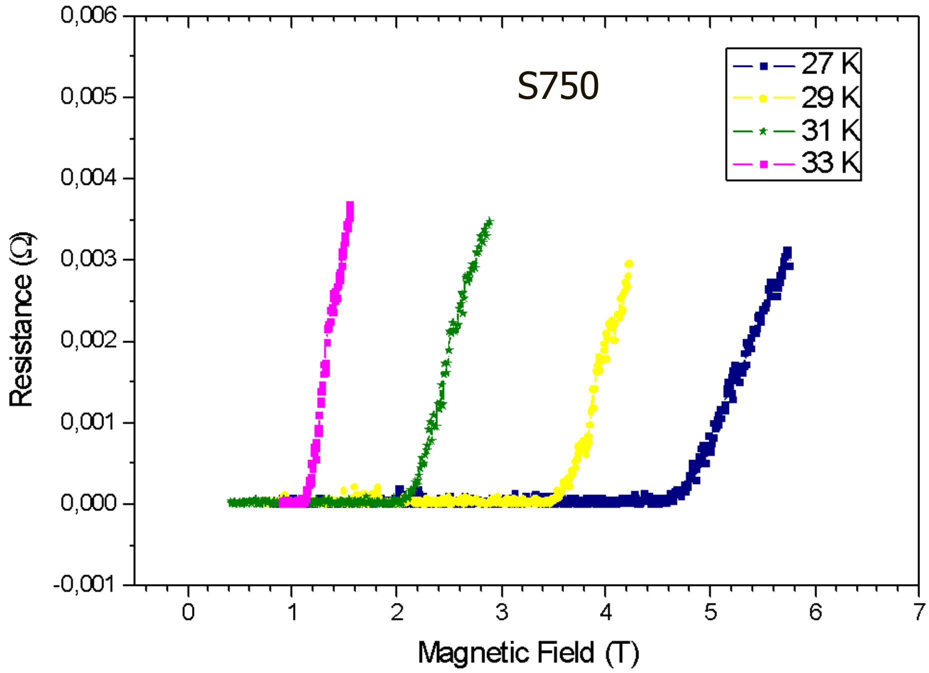
S750
27 K
29 K
31 K
33 K
Resistance (Ω)
Magnetic Field (T)

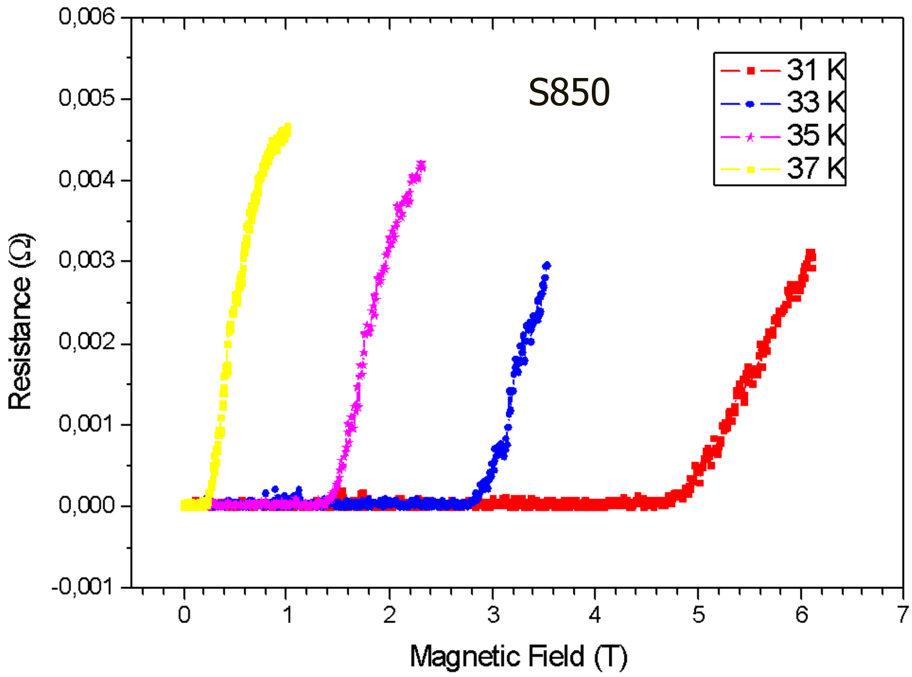
S850
31 K
33 K
35 K
37 K
Resistance (Ω)
Magnetic Field (T)

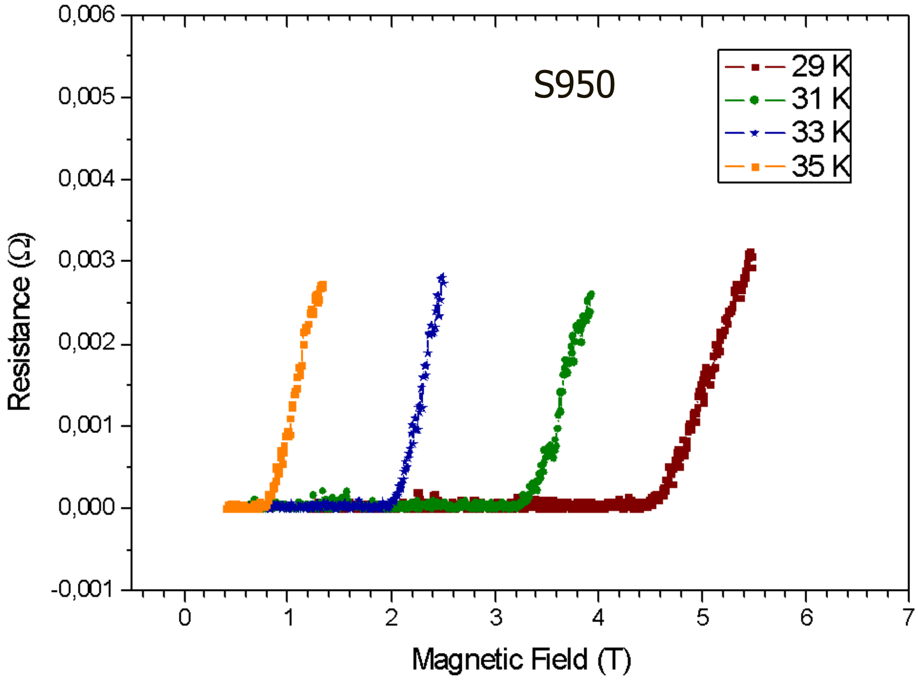

Figure 4.5 *Resistance versus magnetic field graphs for all the samples at constant four different temperatures*

Table 4.4 *The values of critical magnetic field, H_{C2}, for the samples*

S650		***S750***		***S850***		***S950***	
T (K)	***H_{C2} (T)***	***T (K)***	***H_{C2} (T)***	***T (K)***	***H_{C2} (T)***	***T (K)***	***H_{C2} (T)***
26	***4.6***	***27***	***4.8***	***31***	***4.7***	***29***	***4.6***
28	***3.1***	***29***	***3.5***	***33***	***2.8***	***31***	***3.3***
30	***2.1***	***31***	***2.1***	***35***	***1.4***	***33***	***2.0***
32	***1.0***	***33***	***1.2***	***37***	***0.3***	***35***	***0.8***

4.5 The Analysis of AC Susceptibility Measurements

Figure 4.4 shows AC susceptibility versus temperature at various AC field for all the samples. The extracted T_{offset} and T_{onset} values at 240 A/m from the real part of AC susceptibility measurements were listed for each sample in Table 4.5. The T_{offset} at 240A/m AC-magnetic field for the samples S650, S750, S850 and S950 were found to be 38.66, 39.46, 39.85 and 39.66 K, respectively. It is observed that the T_c value exhibits a non-monotonic dependence of the annealing temperature since it is maximized for the S850 sample which in good agreement with the present resistance measurements. It was also observed that the characteristics of the AC-susceptibility curves depend on the annealing temperature and the applied AC field. The superconducting transition width of the S650, S750 and S950 samples is 3 K while that of the S850 sample is 1 K. The bulk nature of superconductivity is confirmed by observation of well-defined single-step transition and large shielding fracture for the S850 sample. The reduction in the width of the AC-susceptibility curve observed in the S850 sample may be due to microstructure changes and increase in the contact area among the superconducting grains induced by the optimum annealing temperatures as confirmed with SEM. This behavior probably reflects the improvement of the coupling between superconducting grains.

In the imaginary part of the AC-susceptibility curves, there are usually two peaks that relate to the intrinsic (intra-grain behavior observed for low amplitudes of the AC-magnetic field) and extrinsic (inter-grain behavior observed for relatively high amplitudes of the AC-magnetic field) properties of the superconducting grains that form the specimen investigated. No intra-grain peak arising from the irreversible motion of vortices inside the grains was obtained in the present work. The loss peak observed in the imaginary part of the ac-susceptibility curves relates to the coupling between neighboring grains (inter-grain behavior) and is suppressed for the S650 sample while it is quite pronounced for all other samples. This peak indicates the maximum hysteresis loss due to inter-grain motion of vortices. As can be seen in Figure 4.5, the real part of the AC-susceptibility curves shifts to higher temperatures and with (i) decreasing ac-magnetic field amplitudes from 1200 to 240 A/m and (ii) increasing annealing temperature from 650 to 850^{o}C while the inter-granular peak of the imaginary part of the AC-susceptibility curves shifts to lower temperatures and broadens as the AC-magnetic field increases from 240 to 1200 A/m. The amount of the shift as a function of AC-field amplitude is proportional to the strength of the pinning force. In addition, the intensity of the imaginary part increases with increasing AC-field amplitude. This is associated with the irreversible flux penetration into the inter-grains of superconducting MgB_2. Moreover, the imaginary part of the AC-susceptibility curves for the S650, S750 and S950 samples shows a slightly broader coupling with a substantial shift to lower temperatures and with smaller amplitude. This result suggests that these samples have a weaker pinning force. On the contrary, the coupling between neighboring grains is strong so that narrower coupling peaks are obtained, ultimately indicating a higher pinning force for the S850 sample. This finding is supported by the peak temperature dependence as a function of AC-magnetic field investigations and the respective J_c calculations were explained as below. Hence, the conclusion based on the results of AC-susceptibility investigations presented here might be that the S850 sample is a better candidate than the S650, S750 and S950 samples, especially in high-field and current-carrying applications.

Table 4.6 tabulates the peak temperature extracted from the imaginary part of AC-susceptibility measurements as a function of applied AC field for all the samples. From the position of the peaks, the inter-granular critical current densities J_c^{inter} at the peak temperatures, T_p, can be evaluated by using Bean's ''loss peak maximum'' method [18-21]. In Figure 4.6, magnetically estimated critical current densities for only inter-grain region at temperatures close to T_c were plotted since there is no intra-grain peaks. The data of Figure 4.6 were obtained as follows: Full flux penetration occurs at the imaginary part of peak maximum value. At T_p, the magnetically estimated $J_c^{inter}$is given by

$$J_c^{inter}(T_p) = {}^{H_{ac}}/_{d}$$

where H_{ac} (H_{App}) and d are the AC-magnetic field amplitude and the thickness of the sample, respectivelySince we produced the thickness of all samples as equal and 1 mm, the intergranular critical current density values were the same for all samples. (Table 4.7)

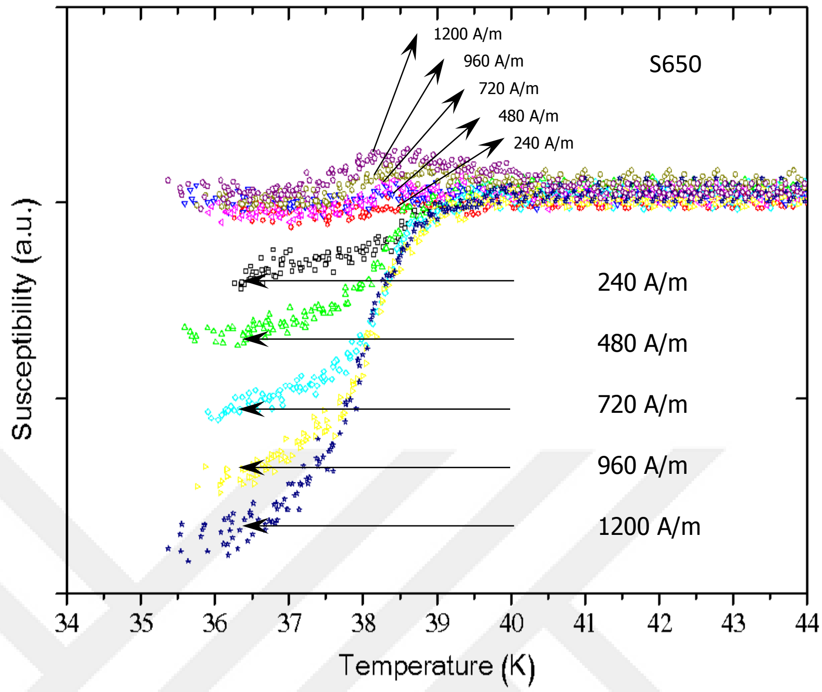
S650
1200 A/m
960 A/m
720 A/m
480 A/m
240 A/m
240 A/m
480 A/m
720 A/m
960 A/m
1200 A/m
Susceptibility (a.u.)
Temperature (K)
34
35
36
37
38
39
40
41
42
43
44

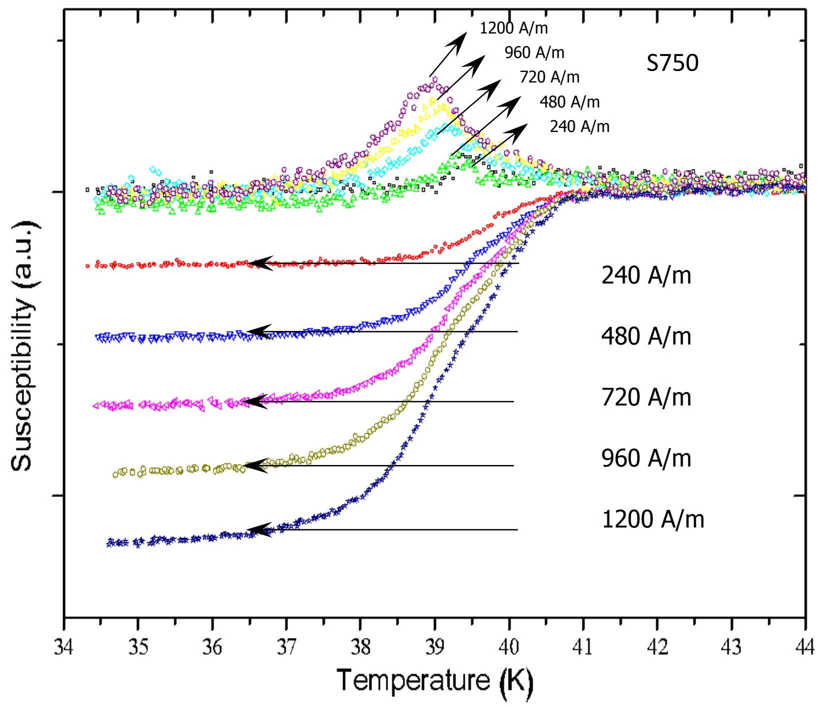
S750
1200 A/m
960 A/m
720 A/m
480 A/m
240 A/m
240 A/m
480 A/m
720 A/m
960 A/m
1200 A/m
Susceptibility (a.u.)
Temperature (K)
34
35
36
37
38
39
40
41
42
43
44

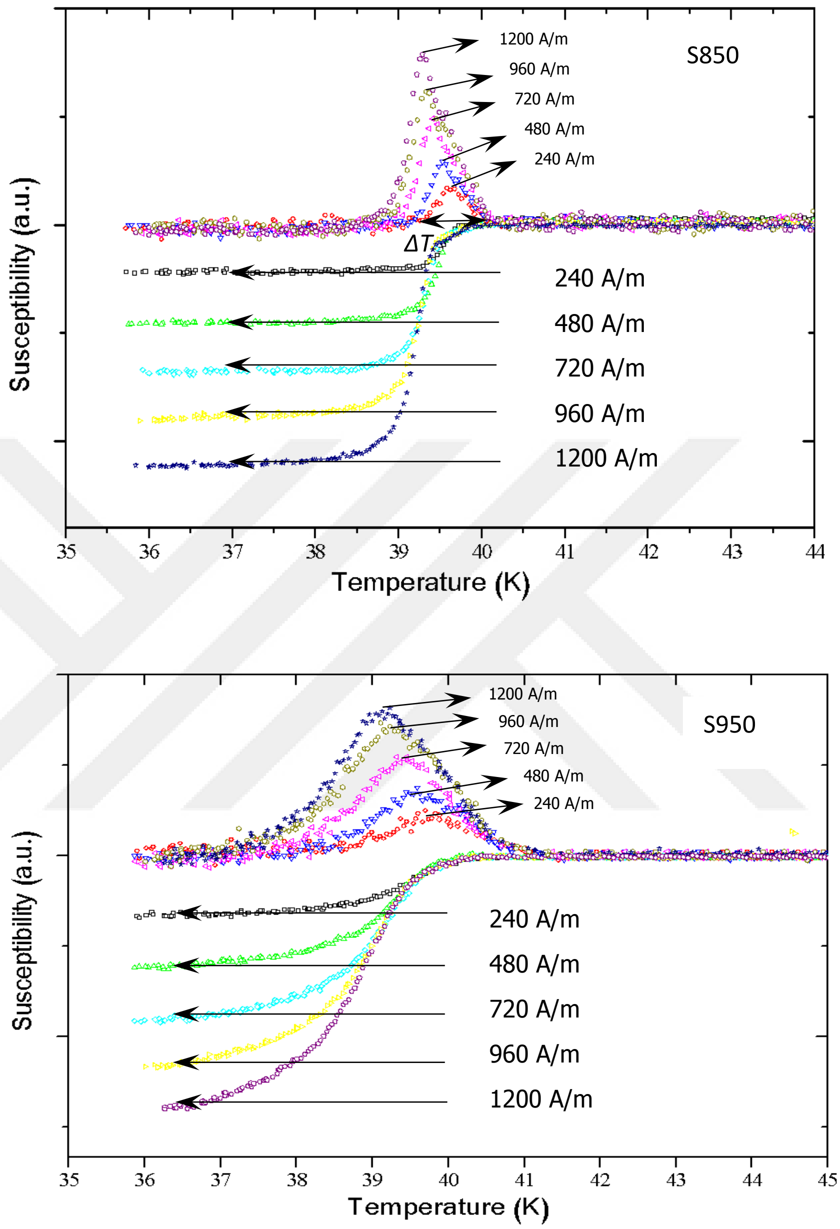

Figure 4.6 *AC-Susceptibility measurements of MgB_2 sample under 240, 480, 720, 960 and 1200 A/m magnetic field for all the samples.*

Table 4.5 *T_{offset} and T_{onset} values at 240 A/m*

Samples	***T_{onset} (K)***	***T_{offset} (K)***
S650	***38.6***	***37.7***
S750	***38.9***	***38.3***
S850	***39.6***	***39.1***
S950	***39.4***	***38.9***

Table 4.6 *The peak temperature as a function of applied AC field for all the samples. H_{App} is the external AC applied magnetic field*

Samples	***S650***	***S750***	***S850***	***S950***
H_{App} (A/m)	***T_P (K)***	***T_P (K)***	***T_P (K)***	***T_P (K)***
240	***38.70***	***39.48***	***39.62***	***39.66***
480	***38.59***	***39.32***	***39.53***	***39.52***
720	***38.48***	***39.19***	***39.42***	***39.38***
960	***38.38***	***39.06***	***39.34***	***39.24***
1200	***38.28***	***38.94***	***39.29***	***39.10***

Table 4.7 *The calculated J_c (T_P) at peak temperatures for all samples*

H_{App} (A/m)	*$J_c(T_p)$ (A/cm^2)*
240	*24*
480	*48*
720	*72*
960	*96*
1200	*120*

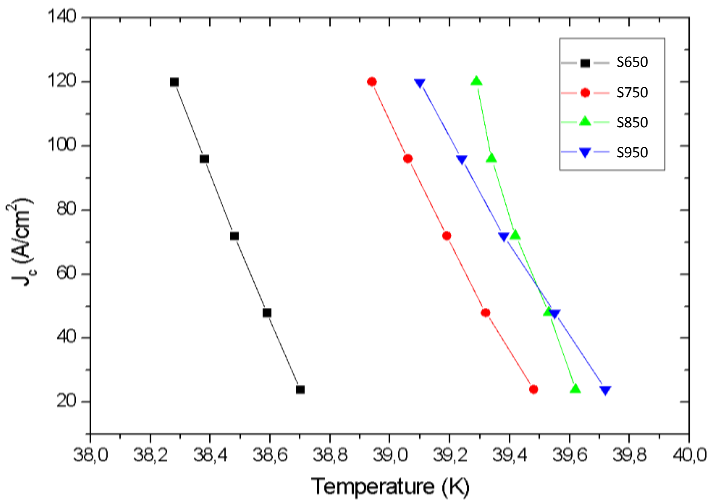

Figure 4.7 *The calculated J_c as a function of peak temperature for all the samples*

J_c was calculated based on the applied area and the thickness of the sample $J_c=H/d$. Since the samples were of the same thickness (d = 1 mm) and the applied areas were equal, J_c was equal for all samples. However, these critical current values are at different peak temperatures for each sample.

5. CONCLUSIONS AND RECOMMENDATIONS

We have studied the microstructure and surface morphology by means of XRD and SEM, the electrical and superconducting properties by means of resistance as a function of temperature and DC magnetic field, and the magnetic behavior by means of the Hall AC-susceptibility method as a function of temperature and AC-magnetic field for the S650, S750, S850 and S950 samples. The findings were listed as following:

1. The increase in annealing temperature up to 850°C promoted the microstructure properties.
2. The lattice parameters and the grain connectivity were worsened while the number and size of voids at surface were worsened with decreasing annealing temperature from 850 to 650°C. The microstructure properties such as grain sizes, denser surface good connectivity between the grains were remarkably enhanced with increasing annealing temperature obtaining their optimum values at 850°C.
3. The superconducting properties such as T_c and ΔT had maximum and minimum values for the S850 sample, respectively. The enhancement of them with increasing the annealing temperature is due to the modification of grain boundaries together with a better crystallinity and larger grains.
4. The higher heat treatment improves the coupling characteristics between superconducting grains, the grain connectivity and these lead to a higher critical temperature and current density. The highest values of inter-grain J_c and T_c were obtained for the S850 sample.
5. From the real and imaginary parts of the AC susceptibility measurements, it is the first time that the anisotropic nature of the MgB_2 compound is revealed by our measurement system in polycrystalline samples.
6. J_c value was the same for all samples. however, it is at different peak temperature values with this value. T_p temperature values at 1200 A/m magnetic field are 38.28, 38.94, 39.29 and 39.10 for S650, S750, S850 and S950 samples, respectively. Therefore, the T_c value depends on the magnetic field and annealing temperature.

Our measurements showed that an increase in the heat treatment up to 850°C enhanced the microstructure, surface morphology, superconducting and magnetic properties of the MgB_2 specimen.

6. REFERENCES

Vancouver citation system was used in this thesis.

1. "Heike Kamerlingh Onnes - Nobel Lecture: Investigations into the Properties of Substances at Low Temperatures, which Have Led, amongst Other Things, to the Preparation of Liquid Helium". Nobelprize.org. Nobel Media AB 2014. Web. 19 Jan 2017. [cited 2022 July 04] Available from: http://www.nobelprize.org/nobel_prizes/physics/laureates/1913/onneslecture.html

2. Onnes, H.K. The Superconductivity of Mercury. Comm. Phys. Lab. Univ., Leiden 1911;122-4.

3. Meissner, W. and Ochsenfeld, R. Einneuer Effektbeieintritt der Supraleitfahigkeit. Naturwissenschaften, 1933; 21:787-8. https://doi.org/10.1007/BF01504252

4. Brauer G. und Esselborn R., Nitridphasen des Niobs, Z. anorg. allg. Chemie 1961;309:151

5. Moshchalkov, V. V.; Menghini, Mariela; Nishio, T.; Chen, Q.; Silhanek, A.; Dao, V.; Chibotaru, L.; Zhigadlo, N.; Karpinski, J.; et al. Type-1.5 Superconductors. Physical Review Letters. 2009;102 (11):117001. doi:10.1103/PhysRevLett.102.117001.

6. Babaev, Egor & Speight, Martin. Semi-Meissner state and neither type-I nor type-II superconductivity in multicomponent systems. Physical Review B. 2005;72(18):180502. doi:10.1103/PhysRevB.72.180502.

7. Abrikosov A.A. On the magnetic properties of superconductors of the second group, Soviet Physics 1957;JETP5:1174

8. Josephson B.D. Possible new effects in superconductive tunnelling. Physics Letter. 1962;Volume 1, Issue 7:251-3 001M. doi:10.1016/0031-9163(62)91369-0

9. Bednorz, J.G., Müller, K.A.: Possible high Tc superconductivity in the Ba-La-Cu-O system. Zeitschrift für Physik B Condensed Matter 1986;64(2):189-93. doi:10.1007/bf01303701

10. Wu, M.K., Ashburn, J.R., Torng, C.J., Hor, P.H., Meng, R.L., Gao, L., Huang, Z.J., Wang, Y.Q., Chu, C.W. Superconductivity at 93 K in a new mixed-phase Y-Ba-Cu-O compound system at ambient pressure. Phys. Rev. Lett. 1987;58(9):908-10. doi:10.1103/PhysRevLett.58.

11. Maeda H.; Tanaka Y.; Fukutumi M. & Asano T.. A New High-Tc Oxide Superconductor without a Rare Earth Element. Jpn. J. Appl. Phys. 1988;27(2):L209–L210. doi:10.1143/JJAP.27.L209.

12. Sheng, Z. Z.; Hermann A. M. Bulk superconductivity at 120 K in the Tl–Ca/Ba–Cu–O system. Nature. 1988;332(6160):138–9. doi:10.1038/332138a0.

13. Nagamatsu, J., Nakagawa, N., Muranaka, T., Zenitani, Y., Akimitsu, J. Superconductivity at 39 K in magnesium diboride. Nature 2001;410(6824):63-4. doi:10.1038/35065039

14. Kamihara, Y., Watanabe, T., Hirano, M. ve Hosono, H. Iron-Based Layered Superconductor La[O1-xFx]FeAs (x = 0.05−0.12) with Tc = 26 K, Journal of the American Chemical Society 2008;130:3296-7 http://dx.doi.org/10.1021/ja800073m

15. Kogan V G, Tanatar M A, Prozorov R, London penetration depth at zero temperature and near superconducting transition. Phys. Rev. B 2020;101:104510

16. Ajay Kumar Saxena. Thermodynamics of Superconductors High-Temperature Superconductors 2.nd ed. Springer-Verlag: 2010 p. 34

17. Zeng, X.H., Pogrebnyakov, A.V., Kotcharov, A., Jones, J.E., Xi, X.X., Lysczek, E.M., Redwing, J.M., Xu, S.Y., Lettieri, J., Schlom, D.G., Tian, W., Pan, X.Q., Liu, Z.K.: In situ epitaxial MgB_2 thin films for superconducting electronics. Nat. Mater. 2002;1(1):35-8 doi:10.1038/nmat703

18. Terzioglu C, Varilci A, Belenli I. Investigation of effect of annealing temperature on mechanical properties of MgB_2. Journal of Alloys and Compounds 2009; Volume 478, Issues 1–2:836-41

19. Varilci A, Yegen D, Revealing the Anisotropy in MgB_2 Superconductor and Investigation of Critical Current near Critical Temperature by Using Hall Probe Susceptibility Technique. J. Supercond. Nov. Magn. 2008;21:451–6

20. Varilci A, Yegen D, Tassi M, Stamopoulos D, Terzioglu C, Effect of annealing temperature on some physical properties of MgB_2 by using the Hall probe ac-susceptibility method. Physica B 2009;404:4054–9

21. Varilci A, Influence of magnetic fields on hysteretic ac losses in bulk MgB2 superconductor investigated by using Hall probe ac susceptibility method. Supercond. Sci. Technol.2007;20:397

22. Vinod, K., Kumar, R.G.A., Syamaprasad, U. Prospects for MgB_2 superconductors for magnet application. Supercond. Sci. Technol. 2007;20(1):R1-R13 doi:10.1088/0953-2048/20/1/r01

23. Xi, X.X. Two-band superconductor magnesium diboride. Rep. Prog. Phys. 2008;71(11):116501 doi:10.1088/0034-4885/71/11/116501

24. Kortus, J. Current progress in the theoretical understanding of MgB_2. Physica C 2007;456(1-2):54-62 doi:10.1016/j.physc.2007.01.023

25. Patel, D., Al Hossain, M.S., Motaman, A., Barua, S., Shahabuddin, M., Kim, J.H. Rational design of MgB_2 conductors toward practical applications. Cryogenics 2014;63:160-5. doi:10.1016/j.cryogenics.2014.04.016

25. Vinod, K., Varghese, N., Syamaprasad, U. Superconductivity of MgB_2 in the BCS framework with emphasis on extrinsic effects on critical temperature. Supercond. Sci. Technol. 2007;20(10):R31-R45. doi:10.1088/0953-2048/20/10/r01

26. Blumberg, G., Mialitsin, A., Dennis, B.S., Zhigadlo, N.D., Karpinski, J. Multi-gap superconductivity in MgB_2: Magneto-Raman spectroscopy. Physica C 2007;456(1-2):75-82. doi:10.1016/j.physc.2007.02.011

27. Ma, Z.Q., Liu, Y.C. Low-temperature synthesis of MgB2 superconductors. Int. Mater. Rev. 2011;56(5-6):267-286 doi:10.1179/1743280411y.0000000002

28. Dimitrov, I.K., Zhang, X., Solovyov, V.F., Chubar, O., Li, Q. Rapid and Semianalytical Design and Simulation of a Toroidal Magnet Made With YBCO and MgB_2 Superconductors. IEEE Trans. Appl. Supercond. 2015;25(5):1-8. doi:10.1109/tasc.2015.2448455

29. Ling, J.Y., Voccio, J.P., Hahn, S., Kim, Y., Song, J.B., Bascunan, J., Iwasa, Y. Construction and Persistent-Mode Operation of MgB_2 Coils in the Range 10-15 K for a 0.5-T/240-mm Cold Bore MRI Magnet. IEEE Trans. Appl. Supercond. 2015;25(3):1-5. doi:10.1109/tasc.2014.2370105

30. Matsmoto A, Kumakara H, Kitaguchi H, Fuji H, Tugano K. The annealing effects of MgB_2 superconducting tapes Physica C 2002;382:207

31. Xu G J, Pinholt R, Bilde-Sorensen J, Grivel J C, Abrahamsen A B, Andersen N H. Effect of starting composition and annealing temperature on irreversibility field and critical current density in Mg_xB_2. Physica C 2006;434:67.

32. Jones M.E, Marsh R E. The Preparation and Structure of Magnesium Boride, MgB2. Journal of the American Chemical Society 1954;76(5):1434-6. doi:10.1021/ja01634a089

33. Oikawa K, Kamiyama T, Mochiku T, Takeya H, Furuyama M, Kamisawa S, Arai M, Kadowaki K. Neutron powder diffraction study on ($Mg_{11}B_2$) synthesized by different procedures. J. Phys. Soc. Jpn. 2002;71(10):2471-6. doi:10.1143/jpsj.71.2471

34. Jorgensen J D, Hinks D G, Short S. Lattice properties of MgB_2 versus temperature and pressure. Phys. Rev. B 2001;63(22) 224522-36. doi:10.1103/PhysRevB.63.224522

35. Evans A F, Wilshaw T R, Quasi-static solid particle damage in brittle solids-I. Observations analysis and implications. Acta Metallurgica 1976;24(10):939-56

36. Drozd V A, Gabovich A M, Gierłowski P, Pezkała M, Szymczak H. Transport properties of bulk and thin-film MgB_2 superconductors: effects of preparation conditions. Physica C 2004;402(4):325-34